JACS
JOURNAL OF THE AMERICAN CHEMICAL SOCIETY
Communication
pubs.acs.org/JACS

New $LaMAsH_x$ (M = Co, Ni, or Cu) Arsenides with Covalent M−H Chains

Hiroshi Mizoguchi,[†] SangWon Park,[†,‡] Haruhiro Hiraka,[§] Kazutaka Ikeda,[§] Toshiya Otomo,[§] and Hideo Hosono*[,†]

[†]Materials Research Center for Element Strategy, Tokyo Institute of Technology, 4259 Nagatsuta, Midori-ku, Yokohama 226-8503, Japan

[§]Institute of Materials Structure Science, High Energy Accelerator Research Organization (KEK), Tsukuba, Ibaraki 305-0801, Japan

Supporting Information

ABSTRACT: A new series of tetragonal LaPtSi-type mixed-anion arsenides, $LaMAsH_x$ (M = Co, Ni, or Cu), has been synthesized using high-temperature and high-pressure techniques. The crystal structure of these intermetallic compounds determined via powder neutron diffraction is composed of a 3D framework of three connected planes with the La ions filling the cavities in the structure. Each late transition-metal ion M, all of which have relatively large electronegativities, behaves like a main group element and forms a planar coordination configuration with three As ions. The trigonal-bipyramidal coordination adopted by the H in the cavity, HM_2La_3, is compressed along the C_3 axis, and unusual M−H chains run along the x and y directions, reinforcing the covalent framework. These chains, which are unique in solids, are stabilized by covalent interactions between the M 4s and H 1s orbitals.

The hydrogen ion has several unique characteristics: its charge can change between +1 and −1; its size is rather flexible, even in the same charge state; it has an isotropic electronic structure due to the lack of energetically available p orbitals; H^- is a strong σ donor with a filled 1s orbital and is comparable to $(CN)^-$; the energy level of its $1s^2$ orbital is fairly changeable; and so on.[1] These features dominate the chemical bonding in hydride crystals. H^- anions commonly form salt-like ionic compounds with electropositive cations, such as alkali, alkali earth, and rare earth ions. H, on the other hand, often forms molecular compounds with main group elements via covalent bonding. Complicated behavior is observed in the reaction of hydrogen with transition metals (TMs), and much research has been devoted to hydrogen storage materials for commercial applications.[2,3] Recently, late TM ions have been attracting attention because they behave as both cations and anions, altering their valence state from positive to negative depending on the local environment,[4] just as is seen with hydrogen. Late TMs with relatively large electronegativities have localized d orbitals because of their large core charges. As a result, the energy levels of their open shell $(n - 1)$d orbitals are comparable to those of their ns orbitals in neutral or negative oxidation states. 5d TM anions including Au^- are commonly observed where the 6s orbitals are contracted and stabilized due to relativistic effects. Unlike heavy TM anions, 3d TM ions must have widespread 4s orbitals in the energy region near the Fermi energy (E_F). Thus, a 3d TM ion with an almost fully occupied d orbital due to electron donation from a positive countercation could behave like a unique main group element with a relatively small work function. These chemical features led us to expect that late TMs would react with hydrogen to form a variety of chemical bonds depending on the local environment. Our ongoing exploration of 3d TM hydrides has now produced a new group, $LaMAsH_x$ (M = Co, Ni, Cu), with a hydrogenated LaPtSi-type structure. These compounds consist of an sp^2-like three-dimensionally connected network ($MAsH_x$) due to the acceptance of electrons from electropositive La. Hydrogen is essential for the synthesis of this family, and the formation of strongly covalent M−H−M chains appears to stabilize the 3D framework.

The synthesis of polycrystalline samples of $LaMAsH_x$ (M = Fe, Co, Ni, Cu, Zn) was attempted via a solid-state reaction at elevated temperatures using a belt-type high-pressure anvil cell. The starting materials included M (99.9%) and LaAs (99.9%). Appropriate amounts of these mixtures were milled in ethanol suspensions for 3 h, dried, and then pressed into pellets. Each pellet was then placed in an h-BN sleeve with a mixture of $Ca(OH)_2$ (95%) and $NaBH_4$ (99%) as a solid hydrogen source.[5] The cell was heated at 1473−1573 K under 2.5−5.0 GPa for 0.5−1.0 h. The chemical compositions of the products were determined using a JEOL JXA-8530F electron microprobe analyzer (JEOL). The hydrogen contents were estimated using thermal desorption spectroscopy (TDS). The crystal structures of the synthesized materials were examined via powder X-ray diffraction (XRD; Bruker D8 Advance TXS) using Cu Kα radiation. For $LaMAsH_x$ (M = Ni and Cu), time-of-flight neutron powder diffraction (TOF-NPD) analyses were performed to determine the position of the H at room temperature (RT). These data were collected with an exposure time of 2 h at NOVA (beamline BL21, a decoupled liquid hydrogen moderator) using a 300 kW spallation neutron source at the Japan Proton Accelerator Complex (J-PARC).[6] The sample was filled in a cylindrical null-scattering $V_{96}Ni_4$ alloy container under a helium atmosphere with an indium washer. Rietveld refinements of the TOF-NPD patterns were performed using a General Structure Analysis System (GSAS) code.[7] The scattering lengths used for La, Ni, Cu, As, and H were 8.24×10^{-13}, 10.3×10^{-13}, $7.72 \times$

Received: October 2, 2014
Published: December 1, 2014

   dx.doi.org/10.1021/ja509965z | J. Am. Chem. Soc. 2014, 136, 17390−17393

10^{-13}, 6.58×10^{-13}, and -3.74×10^{-13} cm, respectively. The dependence of electrical resistivity on temperature was measured over the range from 1.8 to 300 K using the conventional four-probe method with an Ag paste to form the electrical wiring. Magnetization measurements were performed using a vibrating sample magnetometer (Quantum Design). Band structure calculations were performed using the linear muffin-tin orbital (LMTO) method with the atomic sphere approximation (ASA) and combined correction.[8]

When M was changed, the formation of three different families of materials was observed. $La_2Fe_2Se_2O_3$-type (2223-type) hydrides were obtained for M = Ti–Mn, as described in a previous report.[9] While no new compounds were obtained for M = Fe, a new tetragonal phase related to the α-$ThSi_2$-type[2] was confirmed when M = Co, Ni, or Cu. $LaZn_{0.5}AsH_x$ with an AlB_2-type structure[2] was synthesized for M = Zn. The α-$ThSi_2$-type crystal structure is closely related to the AlB_2-type structure because both consist of a planar network.[2] All the pellets of the prepared compounds were black and were confirmed to contain large quantities of H, based on TDS measurements. Therefore, the compounds are rare examples of arsenide-hydrides.[9,10] Notably, attempts to obtain these hydrides without the use of high pressure failed. In addition, high-pressure experiments without the use of the hydrogen source for M = Co–Zn yielded only LaNiAs. This compound was found to adopt the AlB_2-type structure, which was in agreement with that reported by Babizhets'ky et al.[11] It is interesting that band-filling control, which is commonly seen in TM oxides including perovskite oxides, is also apparently possible in the covalent compounds $LaMAsH_x$ by changing M (M = Co, Ni, Cu). The unit cell parameters (lattice constants and unit cell volumes) for the new arsenide-hydrides prepared in this study are provided in Table S1 and Figure S1. It is often difficult to distinguish the space group $I4_1/amd$ for the α-$ThSi_2$-type from $I4_1md$ for the LaPtSi-type with M/As ordering via powder diffraction analysis because they have the same extinction condition.[12] The crystal structure of $LaMAsH_x$ was therefore refined based on the LaPtSi-type structure, considering both the difficulty of the disordering of M/As and the cationic ratio of M/As = 1 (estimated via electron probe microanalysis). The positions of the ions, except for H, were estimated via XRD analysis. The position and content of H in $LaMAsH_x$ (M = Ni, Cu) were determined via TOF-NPD analysis. Results of the Rietveld structure refinements for $LaCuAsH_x$ are given in Figure 1, Table 1, and in the SI CIF file. The structure is shown in Figure 2a, and selected bond distances and angles are listed in Table 2. This structure is composed of a 3D framework consisting of three connected planes, with the La ions filling the cavities in the structure. All of the elements occupy 4a sites. The three As–Cu distances in the plane are 2.43 Å, suggesting a similarity to the local coordination of N in h-BN. Because of the Pt/Si ordering seen in the LaPtSi-type structure, the same ions face each other between neighboring chains through the cavity. H, which has occupancy of 0.78, occupies the central position between the two Cu ions and forms Cu–H chains running along the x or y directions. Although there is a similar position between the two As ions where H could be located, the refinements indicated no occupancy (zero) of H in this position. In addition, the As–As distance between the chains (4.23 Å) is too long for dimer formation. The hydrogen content estimated from the TOF-NPD data, $LaCuAsH_{0.78}$, was close to the value obtained from the TDS analysis results, as shown in Figure 3. It should be noted that hydrogen desorption occurred at relatively higher temperatures, particularly for M = Cu. The results of the structure analysis for $LaNiAsH_{0.69}$ are also shown in Tables 2 and S2, and in the SI CIF file. The electrical resistivity of the $LaCuAsH_{0.78}$ pellet was 1 Ω·cm at 300 K and increased gradually to 7 Ω·cm at 2 K, as shown in Figure S3. The Seebeck coefficient obtained was +0.030 mV/K at 300 K, which revealed that the major carrier was a positive hole.

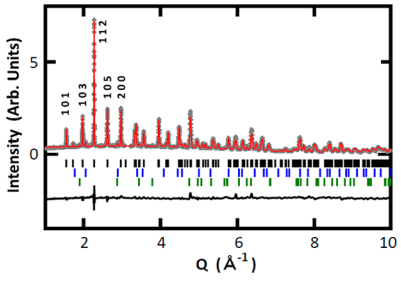

Figure 1. Observed (crosses), calculated (full line), and difference NPD Rietveld profiles for $LaCuAsH_x$ at room temperature. Vertical bars at the bottom show the calculated positions of the Bragg diffractions for $LaCuAsH_x$ (upper), LaAs (middle), and h-BN (lower). The estimated quantities of LaAs and h-BN were 1.5 and 0.2 wt%, respectively.

Table 1. Crystal Structures of $LaCuAsH_x$ As Determined from Rietveld Refinements Based on TOF-NPD Data Sets[a]

atom	site	x	y	z	g	U (Å^2)[b]
La	4a	0	0	0	1	0.0010(3)
Cu	4a	0	0	0.4110(3)	1	0.0016(2)
As	4a	0	0	0.5780(4)	1	0.0016(2)
H	4a	0	0	0.1673(5)	0.78(1)	0.001(1)

[a]The Rietveld refinement (R_{wp} = 6.5%, R_p = 6.0%, $R(F^2)$ = 11.7%) was performed in the space group $I4_1md$ with unit cell parameters of a = 4.23017(5) Å and c = 14.5780(4) Å. [b]The displacement parameters for the Cu and As sites were constrained to be equal.

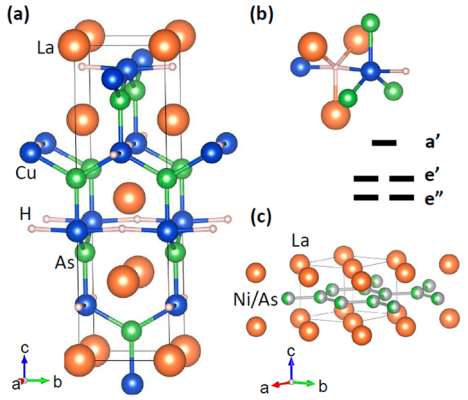

Figure 2. (a) Crystal structure of $LaCuAsH_{0.78}$. (b) Local coordination around Cu and H and schematic energy levels of the Cu 3d orbitals of CuH_2As_3 with D_{3h} symmetry. The principle axis was chosen as the Cu–H direction. (c) Crystal structure of LaNiAs with the AlB_2-type configuration.[11]

Table 2. Structural Features for $LaMAsH_x$

compd	La-H (Å)	M-As (Å)	M-H (Å)	As-M-As (°)	M-H-M (°)
$LaNiAsH_{0.69}$	2×2.374(8)	2×2.407(5)	2×2.0832(3)	119.9(3)	178.4(5)
	2.51(2)	2.44(1)		2×120.1(3)	
$LaCuAsH_{0.78}$	2×2.435(4)	2×2.437(4)	2×2.1171(4)	119.8(1)	175.0(4)
	2.439(8)	2.4235(8)		2×120.5(3)	

dx.doi.org/10.1021/ja509965z | J. Am. Chem. Soc. 2014, 136, 17390–17393

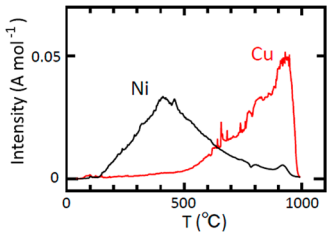

Figure 3. TDS at a specific mass-to-charge ratio, m/z, of 2 (H_2) for $LaMAsH_x$ (M = Ni and Cu).

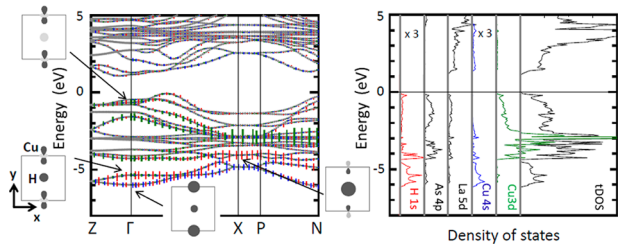

Figure 4. Band structure diagram for LaCuAsH, Γ = (0,0,0), Z = ($^1/_2$,$^1/_2$,$-^1/_2$), X = (0,0,$^1/_2$), P = ($^1/_4$,$^1/_4$,$^1/_4$), and N = (0,$^1/_2$,0). Because this compound belongs to a body-centered tetragonal system, the calculation was performed on the primitive unit cell to minimize the computation time. The Brillouin zone is shown in Figure S4. The binding energy (E = 0) is referenced to the valence band maximum. (Left) Fatband diagram[8] showing the orbital contribution of the Cu 4s (blue), Cu 3d_{z2} (green), and H 1s (red) orbitals. The local orbital coordination system for Cu was defined such that the Cu−H direction in the CuH_2As_3 trigonal-bipyramid (Figure 2b) was chosen as the z-axis. (Right) The PDOS.

The resistivity of $LaNiAsH_{0.69}$ was 2×10^{-3} Ω·cm at 300 K and decreased with T, indicating metallic behavior. No superconducting transition was observed down to 1.8 K. The magnetic susceptibility of $LaCuAsH_{0.78}$ did not exhibit any clear temperature dependence, indicating Pauli paramagnetic behavior due to a minor amount of free carriers.

Figure 4 shows the electronic band structure (E−k diagram) and density of states (DOS) for $LaCuAsH_1$. It can be seen that the valence band maximum is located on the Γ−X line, while the conduction band minimum is located on the Z−Γ line. This result indicates that stoichiometric LaCuAsH should be a semiconductor with an indirect bandgap of ∼1 eV. An investigation of the partial DOS (PDOS, Figure 4, right) provided additional information about the chemical bonds in this compound. The La 4f orbitals are located at approximately +3.8 eV, and the bottom of the conduction band is mainly composed of La 5d and Cu 4s orbitals. In addition, because the As ions tightly coordinate to three Cu ions, the As 4p character is widely distributed in the valence band region (−6 to 0 eV). As shown here, the increased core charge of the element makes the energy level of each outer orbital deeper, resulting in the formation of an M−As covalent bond due to the large energy overlap between the M 3d and As 4p orbitals:

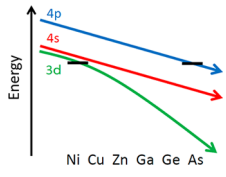

Furthermore, the Cu 3d orbital is nearly fully occupied (∼3d^{10}), and thus spins originating from the 3d orbital are lost. The H 1s orbital also interacts with the Cu 4s3d orbital to form bonding orbitals at approximately −(6.0−4.5) eV. Notably, the bonding parts of the H 1s orbital are deeper than that of the As 4p orbital, suggesting that H serves as a stronger ligand than As. As can be seen in Figure 2b along with the splitting of the 3d orbital in D_{3h} symmetry, CuH_2As_3 adopts a trigonal-bipyramidal coordination configuration that is compressed along the C_3 axis, with Cu−H distances of 2.12 Å and Cu−As distances of 2.43 Å. The short Cu−H distances enhance the destabilization of the a′ (d_{z^2}) orbital. Thus, the local orbital coordination system of Cu is defined such that the Cu−H direction in the CuH_2As_3 trigonal-bipyramid (Figure 2b) is chosen as the z-axis. The E−k diagram (Figure 4, left) contains a fatband description[8] indicated by vertical colored lines and the orbital interactions. The contributions of the H 1s, Cu 4s, and Cu 3d_{z^2} orbitals are represented by red, blue, and green lines, respectively. In the Cu−H chains along the x and y directions, the H 1s orbitals are stabilized to −6.0 eV at the Γ point due to interactions with Cu 4s orbitals as σ donors. As can be seen in the E−k diagram, the width of the valence band at the Γ point is dominated by the orbital interaction between H 1s and Cu 4s 3d_{z^2}. While they cannot mix at the X point due to the translational symmetry, the Cu 4p_z orbital with a shallow energy level can mix slightly. Although the fully occupied Cu 3d does not provide stabilization via the formation of a covalent bond, H-insertion results due to the covalent bond between the Cu 4s−H 1s orbitals. It should also be noted that the obtained sample was found to have a deficiency of H, leading to a lower shift of the E_F and the creation of a positive hole in the valence band, which is consistent with the experimental electrical properties data.

Three types of crystal structures were observed for $LaMAsH_x$ (M = Ti−Zn). It was possible to classify these structures based on the electronegativity of M.[13] For positive M, the H ion acts as a σ donor to form the 2223-type structure. When the electronegativity of M increases from Co to Zn, the M ion behaves like a main group element and forms a covalent MAs network (NW). The addition of excess electrons into the conduction band (antibonding band) of the covalent compounds of main group elements commonly causes bond breaking, resulting in a change in the crystal structure. For example, elemental Si has four available bonding sites and forms a diamond-type structure. However, α-As with an additional electron has three available bonding sites plus a lone pair and thus prefers pyramidal coordination.[2] In $LaMAsH_x$, the crystal structure is maintained as M varies from Co to Cu, indicating that the M ion behaves like a main-group element but retains the characteristics of TM ions. It should be noted that both the 4s and 3d orbitals in these relatively neutral M ions contributed significantly to the formation of the chemical bonds, as indicated by the band structure calculations.

The 3D covalent MAs NW is of particular interest. In the M/As ordered structure, the electrons donated from the positive La are expected to localize on As, judging from the electronegativity of the constituting elements.[13] However, the ionic radius of As^{3-}, ∼2.2 Å,[1] is too large to fit with the observed Cu−As distance of 2.43 Å. It is plausible that ($CuAsH_x$) accepts the donated electrons to form the covalent NW, which is a rare planar net of three connected As ions. This unusual type of coordination for As is also seen in LaRhAs, which has an LaPtSi-type structure,[12c] and LaNiAs, which has an AlB_2-type structure.[11] The formation of the former compound is assisted by the noble character of Rh. The latter compound consists of a graphite-like 2D covalent NW with a Ni−As distance of 2.40 Å (Figure 2c). Electron counting

dx.doi.org/10.1021/ja509965z | J. Am. Chem. Soc. 2014, 136, 17390−17393

results suggest that the NiAs layer ($LaNi^{3-}As$) has an isoelectronic configuration with h-BN with π-bonding. The difficulty in synthesizing LaNiAs[14] suggests a small formation enthalpy for the covalent layer. Here, we attempt to illustrate the effect of the positive La ions from the standpoint of the crystal structure. NiAs adopts a hexagonal structure with octahedral coordination.[2] $LaNi_2As_2$ with a layered $ThCr_2Si_2$-type structure contains an NiAs layer with tetrahedral coordination.[15] Interestingly, with an increase in the content of the reducing agent La, the coordination number of Ni decreases, and the covalency of the NiAs NW increases due to the participation of Ni 4s into the Ni−As bond when going from La_0NiAs (octahedral coordination) to $La_{1/2}NiAs$ (NiAs layer, tetrahedral coordination) to La_1NiAs (planar three-connected network of NiAs). This change is accompanied by stabilization due to the lattice energy in these compounds with charge transfer, $((La_y)^{\delta+}(NiAs)^{\delta-})$. For $LaMAsH_x$ with the LaPtSi-type structure, the contribution of the M−H chains to the stabilization of the MAs NW cannot be ignored. In fact, these compounds were not synthesized without the use of a hydrogen source. While the 3D covalent MAs NW cannot participate in π-bonding because of the long M−As distances, the H ion with dumbbell coordination serves as a graft to reinforce the MAs NW. Using tight binding calculations, Zheng and Hoffmann revealed that direct σ-interactions between the Si $3p_z$ orbitals in the Si net of α-$ThSi_2$-type compounds along the x and y directions, as shown here,

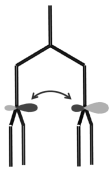

can be ignored because of the long Si−Si distance.[16] It is possible, however, that the interactions proposed by Zheng and Hoffmann are in fact realized by the use of H 1s as the σ donor in $LaMAsH_x$. As−H−As bonds are not observed in these compounds, likely because the As−As distance (4.23 Å) is too short for the incorporation of H.

Finally, the changes in the electronic structure with the change in M from Cu to Co were considered. Figure S1 illustrates a V-shaped curve for the unit cell volumes across the TM series, although the structural parameters do not change significantly, most likely due to the rigid 3D MAs NW. When M changes, E_F shifts to a deeper position due to a decrease in the band-filling. In addition to the H deficiency, the shift gives rise to a positive hole in the valence band, which is an antibonding state of the M 3d−As 4p orbital. Consequently, the M 3d−As 4p bond is strengthened, and the M−As distance is shortened, as shown in Table 2. In fact, metallic electrical properties were observed for $LaNiAsH_{0.69}$ (Figure S3). On the other hand, the decrease in the electronegativity of M from Cu to Co[13] prevents M from behaving like a main-group element. The competition of these effects appears to produce the observed V-shape in the unit cell volumes.

■ ASSOCIATED CONTENT

Supporting Information

Unit cell parameters, neutron powder diffraction, CIF, electrical and magnetic properties, and Brillouin zone. This material is available free of charge via the Internet at http://pubs.acs.org.

■ AUTHOR INFORMATION

Corresponding Author

hosono@lucid.msl.titech.ac.jp

Present Address

‡Advanced Functional Thin Films Department, Korea Institute of Materials Science, Changwon, 641−831, Republic of Korea.

Notes

The authors declare no competing financial interest.

■ ACKNOWLEDGMENTS

This study was supported by the JSPS FIRST project and the JST ACCEL project. We are grateful to Dr. Y. Muraba, S. Jeong, and J. Bang (Tokyo Institute of Technology) for their assistance with the experiments. The neutron scattering experiment was approved by the Neutron Scattering Program Advisory Committee of IMSS, KEK (proposal no. 2014S06). We also thank Profs. O. Jepsen and Y. Nohara (Max Plank Institute, Stuttgart, Germany) for providing us with the LMTO code.

■ REFERENCES

(1) Atkins, P.; Overton, T.; Rourke, J.; Weller, M.; Armstrong, F. *Shriver & Atkins' Inorganic Chemistry*, 5th ed.; Oxford University Press: Oxford, 2009.

(2) Wells, A. F. *Structural Inorganic Chemistry*, 5th ed.; Oxford University Press: Oxford, 1984.

(3) *Hydrogen in Intermetallic Compounds*, Schlapbach, L., Ed.; Springer, Berlin, 1988; Vol. *I*.

(4) Whangbo, M.-H.; Lee, C.; Kohler, J. *Angew. Chem., Int. Ed.* **2006**, *45*, 7465−7469.

(5) Iwamoto, M.; Fukai, Y. *Mater. Trans., JIM* **1999**, *40*, 606−611.

(6) Ohshita, H.; Otomo, T.; Uno, S.; Ikeda, K.; Uchida, T.; Kaneko, N.; Koike, T.; Shoji, M.; Suzuya, K.; Seya, T.; Tsubota, M. *Nucl. Instru. Meth. Phys. Res. A* **2012**, *672*, 75−81.

(7) Larson, A. C.; Von Dreele, R. B. General Structure Analysis System (GSAS) Los Alamos National Laboratory . *Report LAUR 86−748*; Los Alamos National Laboratory: Los Alamos, NM, 2004.

(8) Jepsen, O.; Burkhardt, A.; Andersen, O. K. *Program TB-LMTO-ASA*, version 4.7; Max Planck Institute fur Festorperforschung: Stuttgart, 1999.

(9) Mizoguchi, H.; Park, S.-W.; Hiraka, H.; Ikeda, K.; Otomo, T.; Hosono, H. *Angew. Chem., Int. Ed.* **2014**, DOI: 10.1002/anie.201409023.

(10) (a) Leon-Escamilla, E. A.; Corbett, J. D. *J. Alloys Comp.* **1994**, *206*, L15−L17. (b) Leon-Escamilla, E. A.; Corbett, J. D. *Chem. Mater.* **2006**, *18*, 4782−4792. (c) Muraba, Y.; Matsuishi, S.; Hosono, H. *Phys. Rev. B* **2014**, *89*, 094501/1−6.

(11) Babizhets'ky, V.; Le Senechal, C.; Bauer, J.; Deputier, S.; Guerin, R. *J. Alloys Comp.* **1999**, *287*, 174−180.

(12) (a) Klepp, K.; Parthe, E. *Acta Crystallogr., Sect. B* **1982**, *38*, 1105−1108. (b) Guloy, A. M.; Corbett, J. D. *Inorg. Chem.* **1991**, *30*, 4789−4794. (c) Sologub, O. L.; Salamakha, P. S.; Sasakawa, T.; Chen, X.; Yamanaka, S.; Takabatake, T. *J. Alloys Comp.* **2000**, *345*, L6−L8. (d) Weill, F.; Pasturel, M.; Bobet, J.-L.; Chevalier, B. *J. Phys. Chem. Solids* **2006**, *67*, 1111−1116. (e) Hermes, W.; Rodewald, U. C.; Chevalier, B.; Pottgen, R. *Z. Naturforsch B* **2007**, *62*, 613−616.

(13) Allred, A. L.; Rochow, E. G. *J. Inorg. Nucl. Chem.* **1958**, *5*, 264−268.

(14) The authors of ref 11 have synthesized LaNiAs by the use of arc melting. Although we attempted the synthesis using the same procedure, the reproducibility of the synthesis was not good. It was improved by the aid of high pressure (5 GPa).

(15) Jeitschko, W.; Hofmann, W. K.; Terbuechte, L. J. *J. Less-Common Met.* **1988**, *137*, 133−142.

(16) Zheng, C.; Hoffmann, R. *Inorg. Chem.* **1989**, *28*, 1074−1080.